Cell Biol Toxicol (2024) 40:89
https://doi.org/10.1007/s10565-024-09932-y

RESEARCH

PRDM1 promotes nucleus pulposus cell pyroptosis leading to intervertebral disc degeneration via activating CASP1 transcription

Cheng Yu · Jianjun Li · Wenhao Kuang · Songjia Ni · Yanlin Cao · Yang Duan

Received: 18 June 2024 / Accepted: 16 October 2024 / Published online: 21 October 2024

Abstract Intervertebral disc degeneration (IVDD) is a primary contributor to low back pain and poses a considerable burden to society. However, the molecular mechanisms underlying IVDD remain to be elucidated. PR/SET domain 1 (PRDM1) regulates cell proliferation, apoptosis, and inflammatory responses in various diseases. Despite these regulatory functions, the mechanism of action of PRDM1 in IVDD remains unexplored. In this study, we investigated the role and underlying mechanisms of action of PRDM1 in IVDD progression. The expression of PRDM1 in nucleus pulposus (NP) tissues and NP cells (NPCs) was assessed using western blotting, immunohistochemistry, and immunofluorescence. The effects of PRDM1 on IVDD progression were investigated in vitro and in vivo. Mechanistically, mRNA sequencing, chromatin immunoprecipitation, and dual-luciferase reporter assays were performed to confirm that PRDM1 triggered CASP1 transcription. Our study demonstrated for the first time that PRDM1 expression was substantially upregulated in degenerated NP tissues and NPCs. PRDM1 overexpression promoted NPCs pyroptosis by inhibiting mitophagy and exacerbating IVDD progression, whereas PRDM1 silencing exerted the opposite effect. Furthermore, PRDM1 activated CASP1 transcription, thereby promoting NPCs pyroptosis in vitro. Notably, CASP1 silencing reversed the effects of PRDM1 on the NPCs. To the best of our knowledge, this study is the first to demonstrate that PRDM1 silencing inhibits NPCs pyroptosis by repressing CASP1 transcription, which may be a promising new therapeutic target for IVDD.

Keywords Intervertebral disc degeneration · Pyroptosis · Mitophagy · PRDM1 · CASP1

Abbreviations

HE	Hematoxylin and eosin
IVDD	Intervertebral disc degeneration
LBP	Low back pain
NP	Nucleus pulposus
NPC	Nucleus pulposus cell
AF	Annulus fibrosus
IVD	Intervertebral disc
TNF	Tumor necrosis factor
ROS	Reactive oxygen species
PBS	Phosphate-buffered saline
PIC	Protease inhibitor cocktail
SOFG	Safranin O-Fast Green

Supplementary Information The online version contains supplementary material available at https://doi.org/10.1007/s10565-024-09932-y.

Cheng Yu and Jianjun Li contributed equally to this work.

C. Yu · J. Li · W. Kuang · Y. Cao · Y. Duan (✉)
Department of Spinal Surgery, Zhujiang Hospital, Southern Medical University, Guangzhou 510260, China
e-mail: duanxy@smu.edu.cn

S. Ni
Department of Trauma Orthopaedics, Zhujiang Hospital, Southern Medical University, Guangzhou 510260, China

CCCP Carbonyl cyanide m chlorophenyl hydrazine
DHI Disc height index
GO Gene ontology

Introduction

Low back pain (LBP) is one of the most prevalent global health problems. It substantially affects an individual's quality of life and imposes a considerable economic burden on society (Lyu et al. 2021; Samanta et al. 2023; Wang et al. 2024a, b). Intervertebral disc degeneration (IVDD) is a major contributor to LBP (Fine et al. 2023; Novais et al. 2019). The intervertebral disc comprises a central nucleus pulposus (NP), an outer fibrous annulus, and cartilage endplates located above and below the disc (Liu et al. 2024; Song et al. 2022). IVDD pathogenesis is complex, and excessive cell death and extracellular matrix catabolism of NP are the main pathogenic mechanisms of the disease (Song et al. 2023a, b; Zhou et al. 2023a, b). Despite these insights, the molecular mechanisms underlying IVDD remain poorly understood.

Pyroptosis is a form of programmed cell death triggered by inflammasomes and caspases that leads to the release of inflammatory cytokines(Guo et al. 2023; Yawoot et al. 2023; Zhou et al. 2023a, b). Pyroptosis is closely associated with IVDD development. A20 attenuates NP cell (NPC) pyroptosis by promoting mitophagy and stabilizing mitochondrial dynamics (Peng et al. 2022). Yu et al. reported that BMP7 inhibits NPC pyroptosis and NLRP3 inflammasome activation to ameliorate IVDD in rats (Yu et al. 2023). Zhang et al. demonstrated that inhibiting the activation of the mtDNA-cGAS-STING-NLRP3 axis reduces NPC pyroptosis and attenuates IVDD progression in vivo (Zhang et al. 2022). However, the molecular mechanisms by which pyroptosis promotes IVDD progression remain unknown.

PR domain-containing 1 with zinc finger domain (PRDM1; also known as Blimp-1), a transcription factor, is a DNA-binding protein that recognizes specific target gene sequences and plays a role in the development of many human diseases by activating or inhibiting target gene transcription (Lambert et al. 2018). PRDM1 plays a substantial role in tumor development (Li et al. 2022; Liu et al. 2018), tumor resistance (Kim and Moon 2021), proliferation, immune cell death (Guo et al. (2022) and arthritis regulation (Zhao et al. 2023a). However, the function and potential mechanism of action of PRDM1 in IVDD progression remain unclear.

Herein, we showed that PRDM1 was notably upregulated in both IVDD tissues and cells, as revealed by RNA sequencing, bioinformatics analysis, and validation experiments. Functional assays showed that PRDM1 promoted NPC pyroptosis both in vitro and in vivo. In addition, our data demonstrated that PRDM1 induced caspase 1 (CASP1) expression by directly activating CASP1 transcription. Finally, our data revealed that PRDM1 interacted with CASP1 to inhibit mitophagy in NPCs, thereby exacerbating IVDD progression.

Materials and methods

Human samples and ethics statement

Thirteen NP tissue samples, including control and degenerated NP samples, were collected from patients who underwent lumbar spine surgery for lumbar disc herniation at the Zhujiang Hospital of Southern Medical University. All patients underwent preoperative magnetic resonance imaging (MRI), and the NP tissue was categorized into control (grade I–III) or IVDD groups (grade IV–V) according to the Pfirrmann grading system (Pfirrmann et al. 2001). This study was approved by the Ethics Committee of Zhujiang Hospital of Southern Medical University (2022-KY-117–01), and informed consent was obtained from all the patients. Information on all patients is presented in Supplementary Table S1 table 1.

Cell culture and transfection

NPCs were cultured as previously described (Duan et al. 2023). Following previous studies (Ma et al. 2022), we used interleukin (IL)-1β (*20 ng/mL*; Peprotech) to induce NPC degeneration, carbonyl cyanide m-chlorophenyl hydrazone (CCCP) (10 μM; MedChemExpress) was used to induce mitophagy in NP cells. GenePharma Biotechnology (Suzhou, China) constructed rat CASP1 and negative control siRNAs. The siRNA was transfected according to the manufacturer's instructions. Briefly, NPCs were inoculated into 6-well plates, and 24 h later, 100 pmol

Table 1 Patient information

NO	Gender	Age	Pfirrmann grades	Surgery
1	M	21	1	TLIF
2	M	35	2	TLIF
3	M	23	2	TLIF
4	F	30	3	TLIF
5	M	27	2	TLIF
6	F	74	4	TLIF
7	F	54	4	TLIF
8	F	41	5	TLIF
9	M	83	4	TLIF
10	F	62	5	TLIF
11	F	71	5	TLIF
12	M	45	4	TLIF
13	F	70	5	TLIF

NO. (Number), *M* (male), *F* (female), *TLIF* (Transforaminal Lumbar Interbody Fusion)

Table 2 The sequences of siRNA or shRNA

siRNA	siRNA sequence (5'-3')
Sh-PRDM1-1	GCCCAAAGAAUGUCCCAAATT
Sh-PRDM1-2	GGACCUCGAUGACUUUAGATT
Sh-PRDM1-3	GCAGCAUGAAUGGCAUCAATT
Si-CASP1-1	GUGCGAUCAUGUCACUAAATT
Si-CASP1-2	GUACCUUCCUUGUAUUCAUTT
Si-CASP1-3	GGAUCACAUACUCUAAUGATT
Si-CASP1-4	GCAUUAAGAAGGCCCAUAUTT

of CASP1 siRNA or negative control siRNA was transfected into NPCs with 5-*μL* Lipofectamine 3000 (Invitrogen). Lentivirus (GenePharma) was used to overexpress or silence PRDM1. Lentivirus transfection was performed according to the manufacturer's instructions.

NPCs were infected with LV-PRDM1, LV-NC, Sh-PRDM1, or Sh-NC at a multiplicity of infection of 20. Transfection efficiency was confirmed by RT-PCR, IF staining, and western blotting. The shRNA and siRNA sequences are provided in Supplementary Table S2 table 2.

Western blotting

Protein extraction and western blotting were performed as previously described (Duan et al. 2023). Briefly, proteins were extracted from NP tissues and NPCs by using RIPA buffer (Beyotime, Beijing, China). Subsequently, the proteins were separated by electrophoresis using a 12% SDS-PAGE gel (Beyotime) and transferred to a 0.45-*μm* PVDF membrane (Millipore), followed by blocking with QuickBlock™ blocking solution (Beyotime) for 30 min. The membrane was then incubated with primary antibodies overnight at 4 °C. Subsequently, the cells were incubated with secondary antibodies for 1 h at room temperature. Proteins were detected using a chemiluminescent instrument (UVItec Ltd.). All the antibody information is presented in Supplementary Table S3 table 3.

Table 3 Antibody information

Antibodies human (mouse or rat)	Source	Item No
Anti-GAPDH	Proteintech	Cat No. 60004–1-Ig
Anti-PRDM1	abcam	Cat. No. ab241568
Anti-NLRP3	PTM Bio	Cat. No. PTM-20005
Anti-GSDMD	ImmunoWay	Cat No. YT7991
Anti-ASC	PTM Bio	Cat No. PTM-6894
Anti-CASP1	Proteintech	Cat No. 81482–1-RR
Anti-IL-1β	PTM Bio	Cat. No. ABT-106055
Anti-Beclin1	Proteintech	Cat. No. 11306–1-AP
Anti-Parkin	Proteintech	Cat. No. 66674–1-Ig
Anti-LC3	Proteintech	Cat. No. 14600–1-AP

Immunohistochemistry (IHC)

NP tissues were fixed in 4% paraformaldehyde for 48 h and decalcified for 4 weeks. After paraffin embedding, 5-*μm* sections were cut, deparaffinized, and subjected to antigen retrieval and blocking. The sections were incubated overnight at 4 °C with an anti-PRDM1 primary antibody (1:200, Abcam) and then with a secondary antibody at room temperature for 1 h. 3, 3 -diaminobenzidine (DAB) reagent (Solarbio) was used for visualization, followed by hematoxylin counterstaining. The sections were observed and photographed using a Leica microscope.

Senescence-associated β-galactosidase (SA-β-GAL) staining

SA-β-GAL staining was performed using the SA-β-GAL Staining Kit (Beyotime, C0602). Briefly, the cell culture medium was aspirated and the cells were

Table 4 Sequences of the primers

Gene	Species	Forward	Reverse
GAPDH	human	GCACCGTCAAGGCTGAGAAC	AAGATCAAGTACGAATGCAACG
PRDM1	human	AAGATCAAGTACGAATGCAACG	TGCAAGTCTGACATTTGAAAGG
GAPDH	rat	ACGGCAAGTTCAACGGCACAG	CGACATACTCAGCACCAGCATCAC
PRDM1	rat	CAGCACTGACGGAGCCATGAATC	GCGGGTAAGGAAGGGTCTTGTAAC
CASP1	rat	TTGCCCTTTAGAAATAGCCCAGAAG	TCAACATCAGCTCCGACTCTCC

washed three times with phosphate-buffered saline (PBS). They were then fixed for 15 min at room temperature with SA-β-GAL fixative. After fixation, the cells were washed thrice with PBS, and the staining working solution was incubated overnight at 37 °C. The cells were subsequently observed and images were captured using a microscope (Leica DM2500).

Real-time quantitative -PCR

According to the manufacturer's instructions, RNAex Pro reagent (Acurate Biology, AG21101) was used to extract RNA from NPCs. Reverse transcription was performed using the Evo M-MLV RT Mix kit (Acurate Biology, AG11728). Amplification was performed on an RT-qPCR instrument (Life Technologies, QuantStudio3) using a Premix Pro Taq HS qPCR kit (Acurate Biology, AG11701). Primer sequences are provided in Supplementary Table S4 table 4.

Cell death assay

We assessed the rate of NPC apoptosis using the Annexin V-FITC/PI Apoptosis Detection Kit (Solarbio), following the manufacturer's instructions. Briefly, cells were digested with trypsin and resuspended in 1 × binding buffer. Next, 5 μL of Annexin V-FITC was added, and the mixture was incubated for 10 min at room temperature in the dark. Subsequently, 5 μL of PI was added, and incubation was continued for an additional 5 min at room temperature in the dark. Apoptosis was quantified using flow cytometry (Beckman Coulter).

TUNEL staining (Beyotime, C1086) was performed to assess NPC cell apoptosis. Cells were washed three times with PBS, fixed in 4% paraformaldehyde for 30 min, and permeabilized with 0.3% Triton X-100 for 5 min at room temperature. Subsequently, the cells were incubated with the TUNEL working solution for 60 min at 37 °C in the dark. For tissue sections, deparaffinization was followed by 15-min of incubation with proteinase K at 37 °C. Sections were then rinsed three times with PBS, incubated with TUNEL working solution for 60 min at 37 °C in the dark, and sealed again. Sections were observed and photographed under an immunofluorescence microscope (Nikon Ti2-E).

Cell proliferation

The proliferative capacity of NPC was evaluated using a Cell Proliferation Kit (CCK-8, APExBIO) following the manufacturer's instructions. CCK-8 working solution was added to the culture medium and incubated at 37 °C for 1 h. Optical density was measured at 450 nm using a microplate reader (Biotek).

According to the BeyoClick EDU Cell Proliferation Assay Kit (Beyotime), 10 μmol of EDU working solution was added, and the cells were incubated at 37 °C for 3 h. Cells were then fixed with 4% paraformaldehyde for 15 min, permeabilized with 0.3% Triton X-100 for 15 min, and treated with Click reaction solution for 30 min in the dark. The nuclei were stained with Hoechst 33,342 and observed under a fluorescence microscope (Nikon Ti2-E).

Immunofluorescence staining

The rat intervertebral discs were fixed in 4% paraformaldehyde for 48 h, followed by decalcification for 4 weeks. The discs were then embedded in paraffin, sectioned into 5-μm slices, and subsequently deparaffinized and rehydrated. Antigen retrieval and blocking were performed prior to incubation with the primary antibody at 4 °C overnight. The sections were then incubated with secondary antibody at room temperature in the dark for 1 h. Finally, the sections were sealed and observed under a fluorescence microscope.

Table 5 Sequences of the primers

Gene	Sites	Forward	Reverse
CASP1	1	AAGATGCCACCACTCTCTTCAC	GAAGCGATGTTGGAACTGGGT
CASP1	2	ACAGCAGCACTCCATTACTCAG	CCTGCACCCATGTAAGACGTG
CASP1	3	TGGCTTTGCAGTGTACAGCATC	TGTGAGCTCCCACACAGAGTC

mRNA sequencing and data analysis

RNA (1 μg) was used for library construction and reverse transcription, amplification, and validation. Sequencing was performed on Illumina HiSeq, NovaSeq, or MGI2000 instruments, following the manufacturer's guidelines. Differential expression analyses were conducted using the DESeq2 package, with a Padj threshold of < 0.05, to identify differentially expressed genes. Gene ontology (GO) terms for enriched genes were determined using GOSeq (v1.34.1), and in-house scripts were used to analyze significantly differentially expressed genes in KEGG pathways.

Chromatin immunoprecipitation (ChIP) assay

ChIP assays were performed using the SimpleChIP Kit (#9003, Cell Signaling Technology), according to the manufacturer's instructions. Proteins were cross-linked with DNA by adding 37% paraformaldehyde and incubating at room temperature for 10 min, followed by glycine addition and a 5-min incubation. The cells were washed thrice with PBS and resuspended.

Cells were centrifuged at 4 °C for 5 min at 2000 × g. After discarding the supernatant, the nuclei were resuspended, incubated on ice for 10 min, and centrifuged again. The nuclei were treated with micrococcal nuclease at 37 °C for 20 min to digest DNA into 150–900 bp fragments, followed by EDTA addition to halt digestion.

The supernatant was purified and resuspended. For immunoprecipitation, 2 *μL* rabbit anti-PRDM1 or anti-IgG antibody was added and incubated overnight at 4 °C. ChIP-grade magnetic beads were then added and the mixture was incubated for 2 h. After washing, the DNA was purified and quantified using PCR. Primer sequences for CASP1 are listed in Supplementary Table S5 table 5.

Animal experiments

The rat IVDD model was established as previously described (Duan et al. 2023). Sprague–Dawley (SD) rats purchased from the Guangdong Medical Laboratory Animal Center were randomly divided into sham + LV-NC, sham + LV-PRDM1, IVDD + LV-NC, and IVDD + LV-PRDM1 groups. Eight-week-old SD rats were anesthetized and disinfected with iodine povidone, the discs were exposed via the left lumbar muscle interspace, and the incision was closed after injection of 5 *μL* of lentivirus (1×10^9 TU/*mL*) using a microsyringe. After 2 weeks, the same method was used to expose the intervertebral disc for disc puncture to establish the IVDD model. Eight weeks later, MRI and X-ray examinations were performed, and the rat intervertebral discs were obtained.

X-ray and magnetic resonance imaging (MRI) assays

X-ray and MRI were performed before the rats were euthanized as previously described (Duan et al. 2023; Lin et al. 2021). The intervertebral disc height and the height of the adjacent vertebrae in rats were obtained using DICOM 3.0. IVDD grade in the rats was assessed using the Pfirrmann system. Disc height index (DHI) was calculated by dividing the average of three measurements of intervertebral disc (IVD) height by the length of the adjacent vertebrae, as previously described (Han et al. 2008).

Hematoxylin and eosin (HE) and safranin o-fast green (SOFG) staining

HE and SOFG staining were performed as previously described (Duan et al. 2023). Briefly, intervertebral disc samples were fixed, decalcified, dehydrated, and embedded in paraffin. The samples were subsequently sectioned into 5-*μm* thick slices for HE and SOFG staining. Histological grading of the intervertebral discs was performed as previously described (Tam et al. 2018).

Statistical analysis

Results are expressed as the mean ± standard deviation. All statistical analyses were performed using GraphPad Prism 8.0 (GraphPad Software, La Jolla, CA, USA). Comparisons between two groups were made using the Student's t-test, whereas comparisons involving more than two groups were conducted using one-way analysis of variance, followed by Tukey's post hoc test. Statistical significance was set at $P < 0.05$.

Results

High expression levels of PR/SET domain 1 (PRDM1) in intervertebral disc degeneration (IVDD) tissue and cells

To explore the potential role of PRDM1 in IVDD pathogenesis, we collected 13 NP samples from patients with lumbar disc herniation and determined the PRDM1 expression. The NP samples were classified into control (grade II/III) and IVDD (grade IV/V) groups according to the Pfirrmann grading system (Pfirrmann et al. 2001) (Fig. 1A). HE staining confirmed the degeneration grade of the NP samples, as shown in Fig. 1B. The collagen fibers of the degenerated NP became disorganized and numerous vacuolated cells aggregated.To determine the expression of PRDM1 in NP tissues. PRDM1 expression was notably increased in the IVDD tissues (Fig. 1C). Western blotting results also showed that PRDM1 expression increased in IVDD tissues (Figs. 1D and 1E). Furthermore, we cultured normal and degenerated NPCs and identified their senescent phenotype through SA-β-Gal staining (Fig. 1F). RT-qPCR showed that PRDM1 mRNA expression levels in degenerated NPCs were significantly elevated compared with those in normal NPCs (Fig. 1G). Moreover, IF analysis showed that the fluorescence intensity of PRDM1 in degenerated NPCs dramatically increased (Fig. 1H). To further confirm the relationship between PRDM1 expression and IVDD tissues in SD rats, we obtained control NP (8-week-old) and IVDD (48-week-old) samples. The level of degeneration of the NP tissue was confirmed by HE and SOFG staining (Figs. 1I and 1J). In addition, IF revealed that PRDM1 fluorescence intensity was significantly elevated in degenerated NP tissues of rats compared to that in the control group (Figs. 1K and 1L). The western blotting results were consistent with the IF results (Figs. 1M and 1N), suggesting a positive correlation between PRDM1 expression and the degree of NP degeneration. Collectively, these findings indicate that PRDM1 plays a notable role in the progression of IVDD.

PR/SET domain 1 (PRDM1) promotes nucleus pulposus cells (NPCs) pyroptosis by inhibiting mitophagy

To clarify the specific role of PRDM1 in NPCs, lentiviruses were used to construct the overexpressing and silenced cell lines. We confirmed the overexpression and silencing efficiency of PRDM1 by RT-qPCR (Fig. 2A). PRDM1 overexpression substantially exacerbated IL-1β-induced NPC death, whereas silencing of PRDM1 considerably inhibited IL-1β-induced NPC death (Figs. 2B and C). Flow cytometry confirmed that PRDM1 exacerbated IL-1β-induced NP cell death (Figs. 2D and E). Western blotting results showed that cellular pyroptosis-associated proteins (NLRP3, GSDMD-N, ASC, CASP1, and IL-1β) were involved in the regulation of NPC death by PRDM1 (Figs. 2F and G).

To investigate whether PRDM1 affects NPC proliferation, we performed EDU staining and CCK-8 assay. The results showed that PRDM1 substantially inhibited NPC proliferation; however, silencing PRDM1 yielded the opposite results (Figs. 2H–J). Mitophagy regulates cellular pyroptosis in different diseases (Luo et al. 2023; Ma et al. 2022; Xia et al. 2022), and western blotting results confirmed that PRDM1 inhibits mitophagy in NPCs (Figs. 2K and L). Treatment of NPC with CCCP partially reversed the inhibitory effect of PRDM1 on mitophagy (Fig. 2M). Immunofluorescence staining revealed that CCCP rescued mitophagy in the NPCs (Fig. 2N). In summary, we found that PRDM1 exacerbated pyroptosis by inhibiting NPC mitophagy.

PR/SET domain 1 (PRDM1) overexpression exacerbates intervertebral disc degeneration (IVDD) progression in vivo

To further elucidate the role of PRDM1 in IVDD progression, we evaluated the effects of PRDM1 overexpression in rats following the in situ injection of LV-PRDM1 or LV-NC. We performed in situ lentivirus injections in rats at 8 weeks. Two weeks later, an

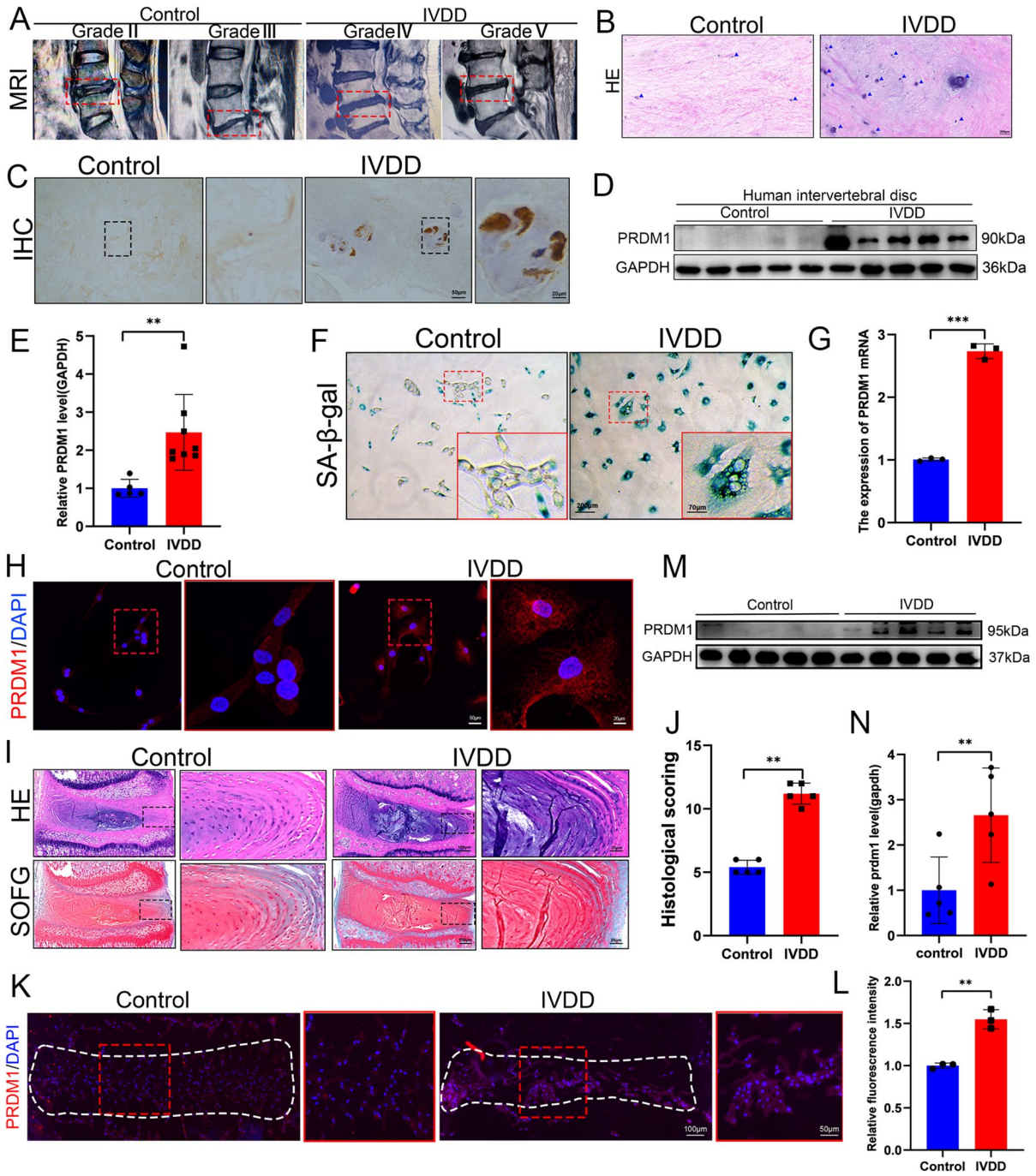

Fig. 1 High expression of PRDM1 in IVDD tissue and cells. (**A**) Representative MRI images of lumbar intervertebral discs with different levels of degeneration. (**B**) HE staining of control and IVDD tissues. (**C**) IHC staining of control and IVDD tissues. (**D**, **E**) Western bolt assay and quantitative analysis of control and IVDD tissues. (**F**) SA-β-gal staining of control and degenerate NPCs. (**G**) RT-qPCR was performed to detect PRDM1 expression levels in control and degenerate NPCs. (**H**) IF staining to detect PRDM1 expression in control and degenerate NPCs. (**I**, **J**) HE and SOFG staining and histologic scoring of control and degenerate rats NP. (**K**, **L**) IF staining and quantitative analysis of control and degenerate rats NP. (M, N) Western blot detection and quantification of control and degenerate rats NP. $^{**}P < 0.01$, $^{***}P < 0.001$

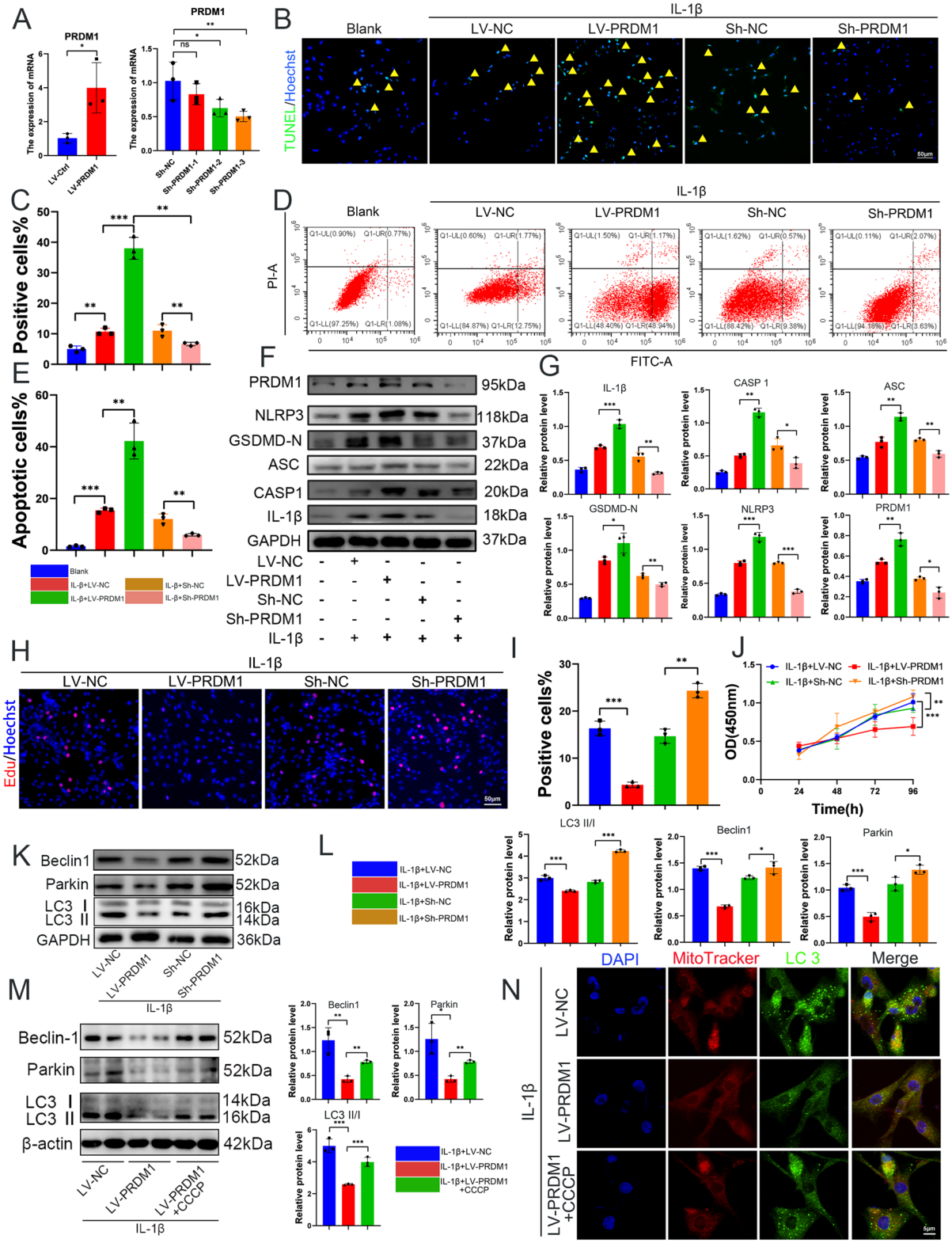
A
PRDM1
The expression of mRNA
LV-Ctrl
LV-PRDM1
Sh-NC
Sh-PRDM1-1
Sh-PRDM1-2
Sh-PRDM1-3
B
IL-1β
Blank
LV-NC
LV-PRDM1
Sh-NC
Sh-PRDM1
TUNEL/Hoechst
C
Positive cells%
D
PI-A
FITC-A
E
Apoptotic cells%
Blank
IL-β+LV-NC
IL-β+LV-PRDM1
IL-β+Sh-NC
IL-β+Sh-PRDM1
F
PRDM1 95kDa
NLRP3 118kDa
GSDMD-N 37kDa
ASC 22kDa
CASP1 20kDa
IL-1β 18kDa
GAPDH 37kDa
G
IL-1β
CASP 1
ASC
GSDMD-N
NLRP3
PRDM1
Relative protein level
H
Edu/Hoechst
I
Positive cells%
J
OD(450nm)
Time(h)
K
Beclin1 52kDa
Parkin 52kDa
LC3 I 16kDa
LC3 II 14kDa
GAPDH 36kDa
L
M
Beclin-1 52kDa
Parkin 52kDa
LC3 I 14kDa
LC3 II 16kDa
β-actin 42kDa
LV-PRDM1 +CCCP
N
DAPI
MitoTracker
LC 3
Merge

◂**Fig. 2** PRDM1 promotes NPCs pyroptosis by inhibiting mitophagy. (**A**) RT-qPCR validation of PRDM1 silencing and overexpression efficiency. (**B**, **C**) TUNEL staining and statistical analysis results of TUNEL-positive cells, scale bar, 50 μm. (**D**, **E**) Flow cytometry analysis of the effects of PRDM1 overexpression and silencing on the death of NPCs. (**F**, **G**) Western blot detection and quantification of pyroptosis-related proteins (NLRP3, GSDMD-N, ASC, CASP1, IL-1β). (**H**, **I**) Edu analyzes the effect of PRDM1 on the proliferation of NPCs, scale bar, 50 μm. (**J**) CCK-8 analyzes the role of PRDM1 on the proliferation of NPCs (**K**, **L**) Western blot detection of mitophagy-related proteins (LC3, Parkin, Beclin1) (**M**) Western blot detection of CCCP (10umol) rescued overexpressing PRDM1 NPCs mitophagy. (**N**) Immunofluorescence analysis of mitophagy staining in PRDM1 overexpression and CCCP-treated NPCs, scale bar, 5 μm. * $P<0.05$, ** $P<0.01$, *** $P<0.001$

IVDD model was established by using an IVD needle stab. Eight weeks later, radiography, MRI, and sample collection were performed (Fig. 3A). X-rays showed that PRDM1 overexpression substantially reduced disc height in the sham-operated group. In addition, PRDM1 overexpression substantially reduced the disc height in the IVDD model group, whereas the adjacent vertebrae showed remarkable osteophytes (Fig. 3B). LV-PRDM1 rats had lower DHI scores than LV-NC rats (Fig. 3C). MRI provided a clearer picture of the disc degeneration level, showing that PRDM1 overexpression resulted in a substantially reduced signal in the intervertebral discs of the sham-operated group and that PRDM1 overexpression resulted in a considerable reduction in the IVDD model group disc signal (Fig. 3D). The Pfirrmann scores in LV-PRDM1 rats were notably lower than those in LV-NC rats (Fig. 3E). HE and SOFG staining showed that the degenerated discs exhibited NP and annulus fibrosus cleft atrophy (Fig. 3F). However, the degenerative disc changes in PRDM1-overexpressing rats were more severe, as evidenced by the disappearance of the boundary between the NP and annulus fibrosus (AF), smaller NP, and increased hypertrophy of the annulus fibrosus (Fig. 3F). The histological scores of intervertebral discs in PRDM1-overexpressing rats were substantially higher than those in the control rats (Fig. 3G). TUNEL staining revealed that PRDM1 overexpression aggravated NP cell death in rats (Fig. 3H and 3I). IF revealed that the in situ injection of PRDM1 lentivirus effectively upregulated PRDM1 expression, and PRDM1 overexpression substantially induced pro-pyroptosis proteins (NLRP3, IL-1β, CASP1, and GSDMD) (Figs. 4A and 4B). Therefore, PRDM1 aggravated IVDD progression in rats by promoting pyroptosis in the NPCs.

Mitophagy is a critical factor for cellular pyroptosis initiation (Luo et al. 2023; Xia et al. 2022). To clarify whether mitophagy is involved in PRDM1-regulated pyroptosis, we performed immunofluorescence on rat intervertebral discs, which showed that PRDM1 overexpression substantially inhibited LC3, Beclin1, and Parkin expression (Figs. 4C and 4D), indicating that PRDM1 overexpression inhibited mitophagy in rat intervertebral discs. In conclusion, PRDM1 aggravated IVDD by inhibiting mitophagy and promoting cellular pyroptosis in vivo.

PR/SET domain 1 (PRDM1) directly activates CASP1 transcription in nucleus pulposus cells (NPCs)

To further elucidate the potential mechanisms by which PRDM1 exacerbates IVDD progression, RNA sequencing (RNA-seq) was performed to identify the downstream target genes of PRDM1. Compared to the control group, the heatmap and volcano plot indicated that 321 genes were downregulated and 676 were upregulated in the PRDM1 overexpression group (Figs. 5A−5C). GO analysis indicated that the functions of these differentially expressed genes were primarily enriched in processes related to the positive regulation of NFκB transcription, positive regulation of tumor necrosis factor (TNF) secretion, and various aspects of interferon and immune responses (Fig. 5D). KEGG analysis revealed that the functions of these differentially expressed genes were primarily enriched in the ferroptosis, rheumatoid arthritis, and sphingomyelin signaling pathways (Fig. 5E). To screen for candidate target genes, we predicted potential target genes of PRDM1 using the Chip-Atlas and hTFtarget online databases. The Venn diagram shows the intersection of the Chip-Atlas, hTFtarget, and RNA-seq candidate target genes (Fig. 5F). The GEPIA2 online database was used to analyze the correlation among the top five candidate target genes (*TLR3, PMAIP1, CASP1, CASP16*, and *IFIT2*) with *PRDM1*. The Spearman's correlation factor between PRDM1 and CASP1 ($R=0.65$, $P<0.05$) revealed a strong correlation (Fig. 5G). RT-PCR results showed that PRDM1 positively regulated CASP1 expression (Fig. 5H). The Jasper database predicted potential sites for PRDM1 and CASP1 (Fig. 6A). We confirmed that

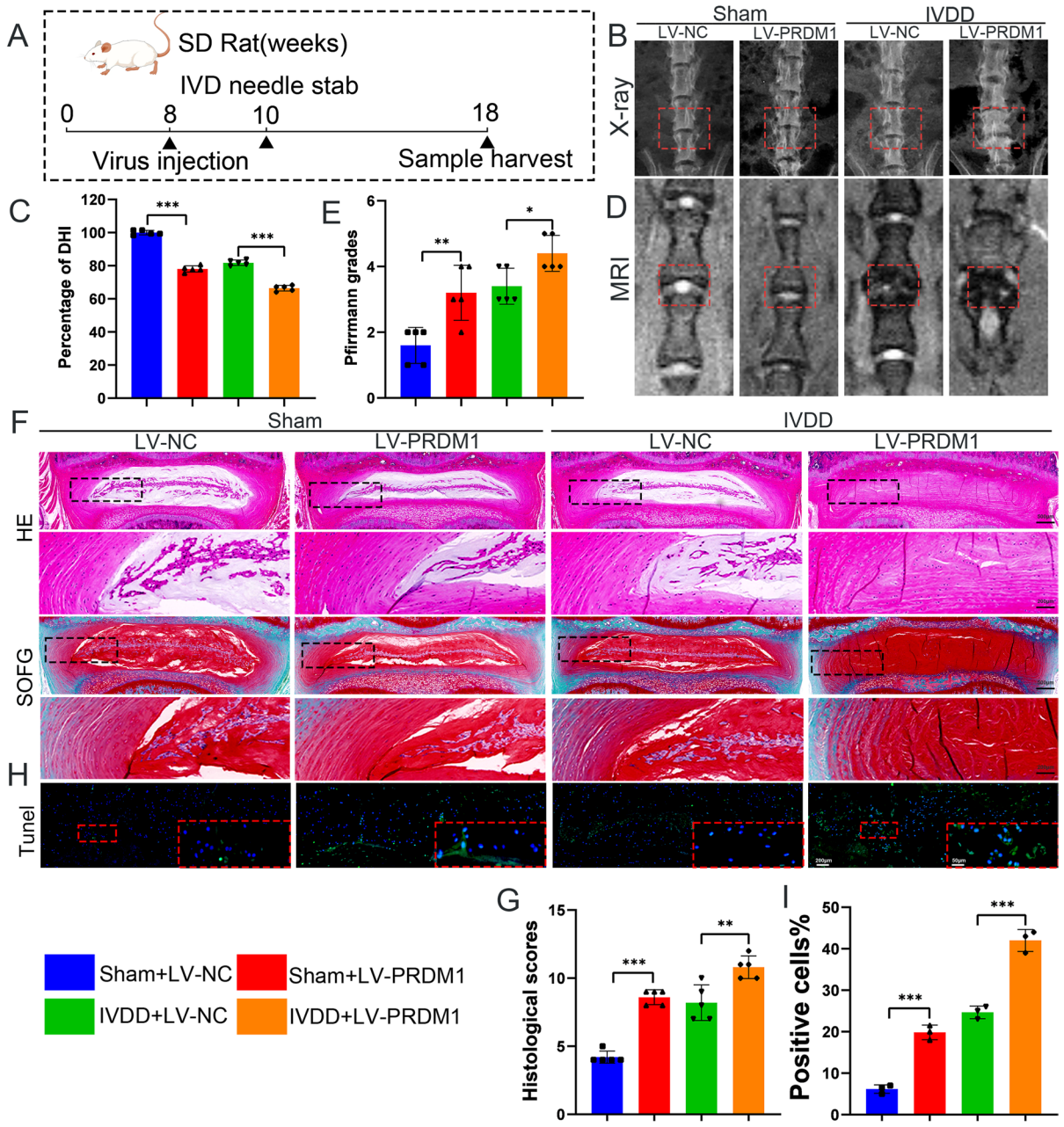

Fig. 3 PRDM1 overexpression exacerbates IVDD progression in vivo. (**A**) Experimental Scheme. Lentivirus was injected into the intervertebral disc 2 weeks before IVD needle stab, and further MRI and X-ray were performed to detect the degree of IVD degeneration. (**B**-**E**) X-ray, MRI and DHI, Pfirrmann score of Rat IVD in LV-NC and LV-PRDM1 group rats, which were treated with or without INS, n = 5. (**F**, **G**) HE and SOFG staining and histologic scoring of IVD in LV-NC and LV-PRDM1 group rats treated as in (B), n = 5, scale bar, 500 μm or 200 μm. (**H**, **I**) TUNEL staining and quantitative analysis of rat IVD in LV-NC and LV-PRDM1 groups treated as in (B), n = 3, scale bar, 200 μm or 50 μm. $^{*}P < 0.05$, $^{**}P < 0.01$, $^{***}P < 0.001$

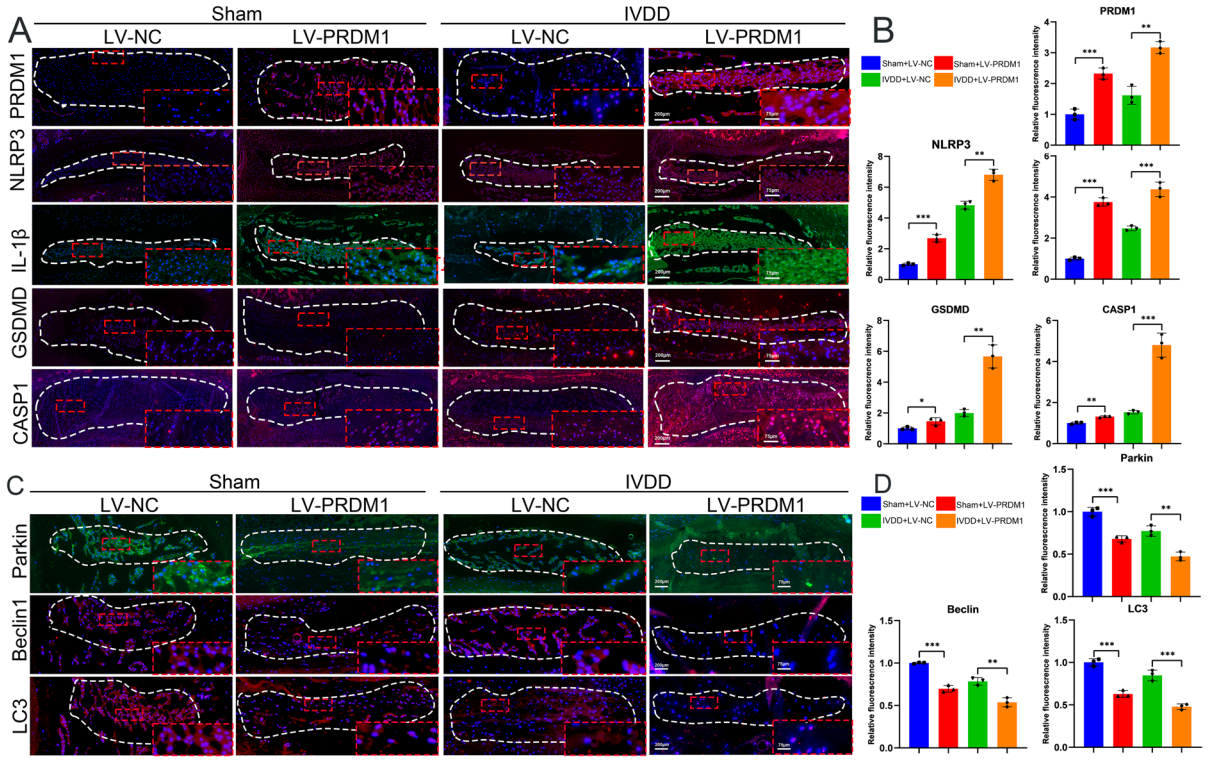

Fig. 4 PRDM1 overexpression exacerbates intervertebral disc pyroptosis by inhibiting mitophagy in rats. (**A**, **B**) Immunofluorescence staining detected and quantified pyroptosis-related proteins (NLRP3, GSDMD-N, ASC, CASP1, IL-1β) in the IVD of LV-NC and LV-PRDM1 rats treated as in (Fig. 3B), n = 3. (**C**, **D**) Immunofluorescence staining detected and quantified mitophagy-related proteins (LC3, Beclin1, Parkin) in the IVD of LV-NC and LV-PRDM1 rats treated as in (Fig. 3B), n = 3, scale bar, 200 μm or 75 μm, $^{*}P < 0.05$, $^{**}P < 0.01$, $^{***}P < 0.001$

PRDM1 binds to the CASP1 promoter region sites 1 and 3 using ChIP assays (Fig. 6B and 6C). Similarly, western blotting revealed a positive regulatory relationship between PRDM1 and CASP1 at the protein level (Figs. 6D and 6E). Finally, using dual-luciferase reporter gene assays, we verified that PRDM1 binds to CASP1 at sites 1 and 3 (Figs. 6F and 6G).

PR/SET domain 1 (PRDM1) promotes nucleus pulposus cells (NPC) pyroptosis via activating CASP1 transcription

First, we confirmed the silencing efficiency of si-CASP1 using western blotting (Fig. 7A). Our results revealed that CASP1 silencing reversed the inhibitory effects of PRDM1 overexpression on NPC proliferation (Figs. 7B−D). Furthermore, TUNEL staining revealed that PRDM1 promoted NPC death, whereas CASP1 silencing dramatically reversed this effect (Figs. 7E and F). Consistently, flow cytometry results revealed that CASP1 silencing reversed the pro-pyroptotic effects of PRDM1 (Figs. 7G and H). Western blotting demonstrated that the elevated expression of pyroptosis-related proteins (NLRP3, GSDMD-N, and IL-1β) induced by PRDM1 overexpression was reversed by CASP1 silencing (Figs. 7I and J). Furthermore, our data revealed that silencing of CASP1 substantially reversed the effect of PRDM1 overexpression on the protein expression of mitophagy-related markers (LC3, Beclin1, and Parkin) in NPCs (Figs. 7K and L). Immunofluorescence revealed that silencing of CASP1 improved the inhibitory effect of PRDM1 on NPC mitophagy (Fig. 7M). Our data demonstrated that PRDM1 inhibited mitophagy by directly activating CASP1 transcription and exacerbating NPC pyroptosis.

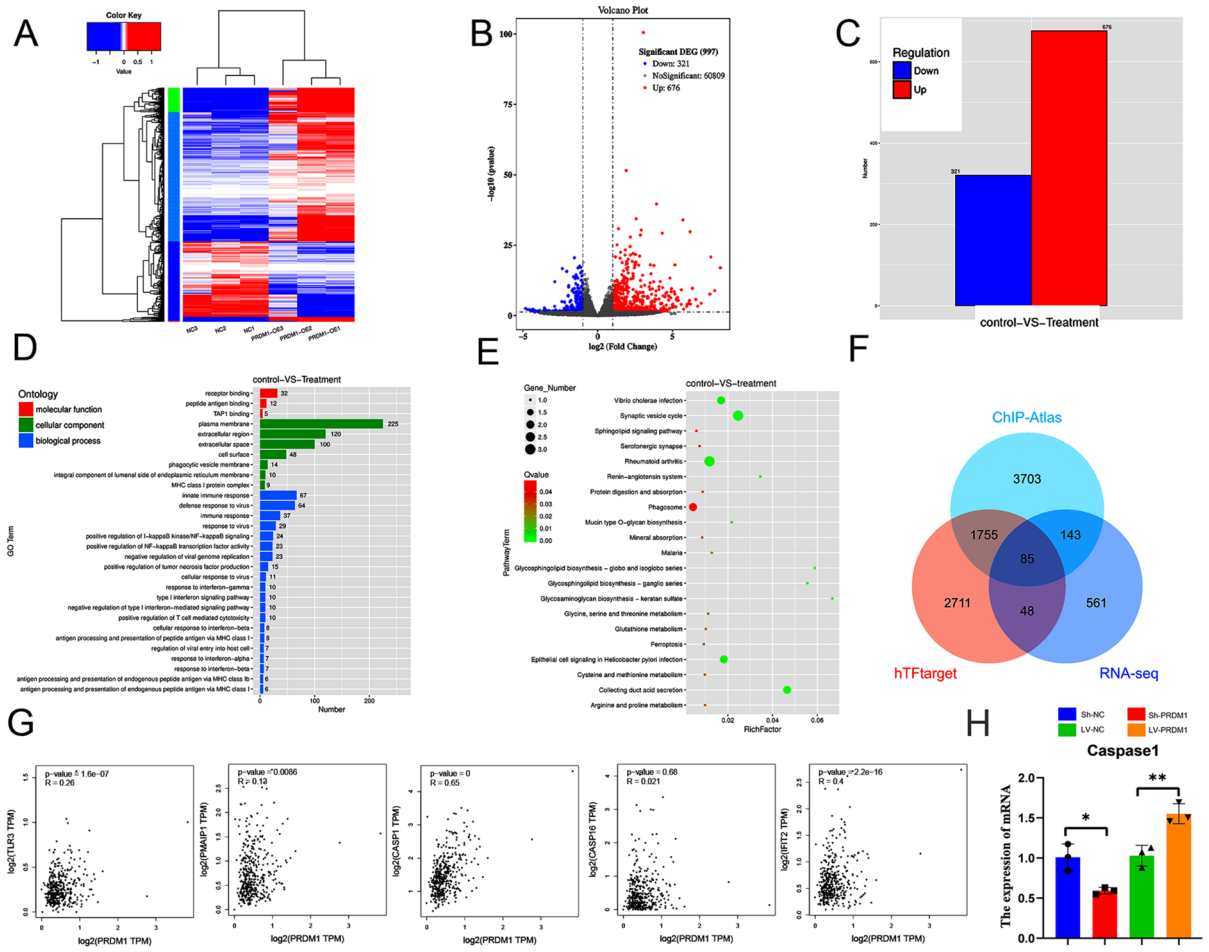

Fig. 5 RNA sequencing to identify PRDM1 downstream target genes. (**A**) Heatmap of differential genes in OE-NC and OE-PRDM1 NPCs. (**B**, **C**) Volcano plots and Statistical map of differential genes in OE-NC and OE-PRDM1 NPCs (up-regulated: 676, down-regulated: 321). (**D**, **E**) GO and KEGG analysis of differential genes in OE-NC and OE-PRDM1 NPCs. (**F**) Chip-Atlas, hTFtarget and RNA-seq potential target gene intersection Venn diagrams. (**G**) Correlation analysis of PRDM1 with potential target genes (TLR3, PMAIP1, CASP1, CASP16 and IFIT2) analyzed by GEPIA database. (**H**) RT-qPCR detection of CASP1 expression levels after overexpression of PRDM1 in NPCs. $^{*}P < 0.05$, $^{**}P < 0.01$

Discussion

Although it is generally accepted that IVDD is associated with apoptosis, senescence, and catabolism in the ECM of NPCs (Clouet et al. 2019; Francisco et al. 2022; Xin et al. 2022), the specific underlying molecular mechanisms remain unclear. To our knowledge, this is the first study to show that PRDM1 accelerates NPC pyroptosis and exacerbates IVDD progression by activating CASP1. Therefore, PRDM1 plays a significant role in the progression of IVDD and represents a potential therapeutic target.

PRDM1, a transcription factor, is believed to play a crucial role in the regulation of cell proliferation (Li et al. 2022; Liu et al. 2018; Martins et al. 2008; Wang et al. 2013). Furthermore, PRDM1 is a crucial molecule for the regulation of cellular inflammatory responses (Zhao et al. 2023) and ferroptosis (Ma et al. 2024). However, the role of PRDM1 in IVDD remains unclear. Our results demonstrated that PRDM1 expression was increased in human degenerated NP tissues, NPCs, and rat IVDD tissues. Therefore, we investigated whether PRDM1 regulates IVDD progression. NPC apoptosis, pyroptosis,

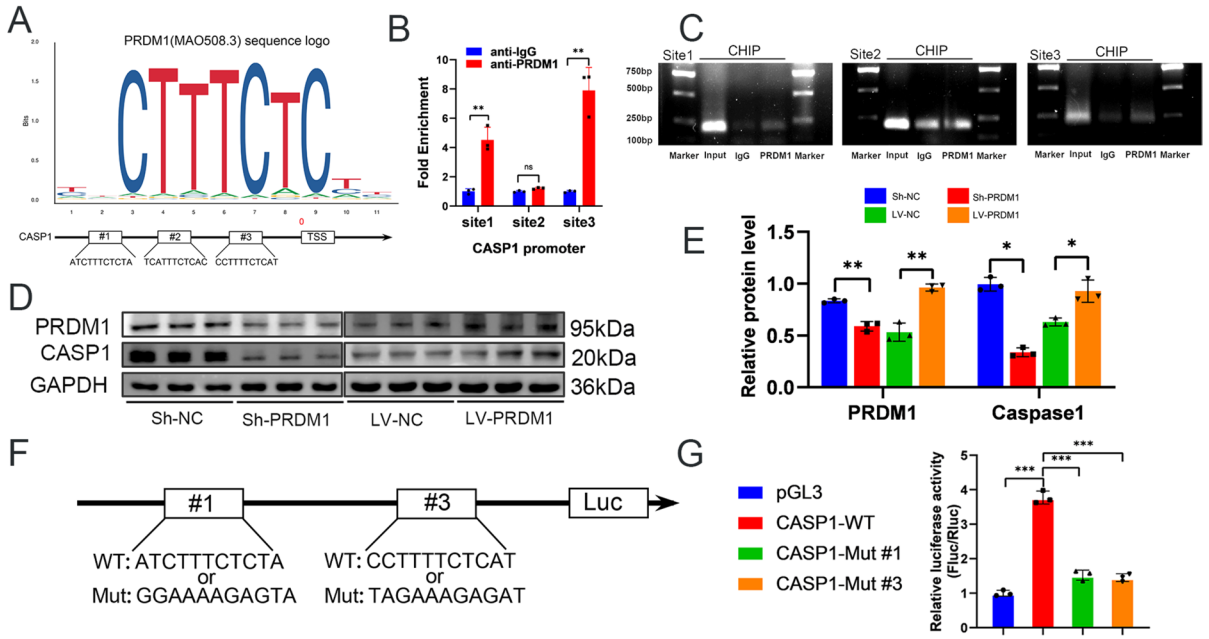

Fig. 6 PRDM1 directly activates CASP1 transcription in NPCs. (**A**) JASPAR predicts the DNA-binding motifs of PRDM1 and possible binding sites for PRDM1 in the CASP1 promoter. (**B**, **C**) ChIP-PCR experiments detected the interaction between the CASP1 promoter and PRDM1. (**D**, **E**) Western blot detected CASP1 protein expression in sh-PRDM1 or LV-PRDM1 NPCs. (**F**, **G**) Luciferase reporter gene assays confirmed that PRDM1 binds to the CASP1 promoter at sites #1 and #3. $^{*}P < 0.05$, $^{**}P < 0.01$, $^{***}P < 0.001$

oxidative stress, and extracellular matrix catabolism are critical factors in exacerbating IVDD (Wang et al. 2024a, b; Zhong et al. 2024). The results revealed that PRDM1 overexpression promoted NPC death and inhibited NPC proliferation. PRDM1 overexpression induced the expression of protein markers of cellular pyroptosis (NLRP3, GSDMD-N, ASC, CASP-1, and IL-1β). In rats, we found that PRDM1 overexpression considerably accelerated IVDD progression while promoting pyroptosis-related protein expression, suggesting that PRDM1 overexpression promoted NPC pyroptosis, revealing the unknown role of PRDM1 in regulating NPC pyroptosis and IVDD progression.

Pyroptosis is a newly identified form of inflammatory cell death that is mediated by inflammasomes. Activation of pyroptosis induces NPC death, ECM catabolism, and inflammatory response, thereby exacerbating IVDD progression (Xing et al. 2021; Zhao et al. 2021; Zhou et al. 2023a). Mitophagy maintains mitochondrial stability by eliminating damaged mitochondria, mitochondrial reactive oxygen species (ROS), and inflammasomes, thereby inhibiting the activation of cellular pyroptosis (Liu et al. 2022; Luo et al. 2023; Peng et al. 2022; Song et al. 2023a, b). However, the specific mechanism by which mitophagy regulates pyroptosis in NPC remains unclear. Therefore, we explored whether PRDM1 regulates NPC pyroptosis by modulating mitophagy. The results indicated that PRDM1 overexpression significantly suppressed the expression of mitophagy-related proteins including LC3, Parkin, and Beclin1. Furthermore, our findings demonstrated that CCCP reversed the inhibitory effect of PRDM1 on mitophagy. The results of the in vivo experiments revealed that PRDM1 substantially aggravated IVDD in rats. Regarding the molecular mechanism, PRDM1 induced the expression of CASP1, GSDMD, IL-1β, and NLRP3 and suppressed the expression of LC-3, Beclin1, and Parkin in rat intervertebral discs. Collectively, these results suggest that PRDM1 exacerbates NPC pyroptosis by inhibiting mitophagy both in vitro and in vivo.

Transcription factors participate in biological processes by activating or repressing downstream target genes (Chen et al. 2013; Lai et al.

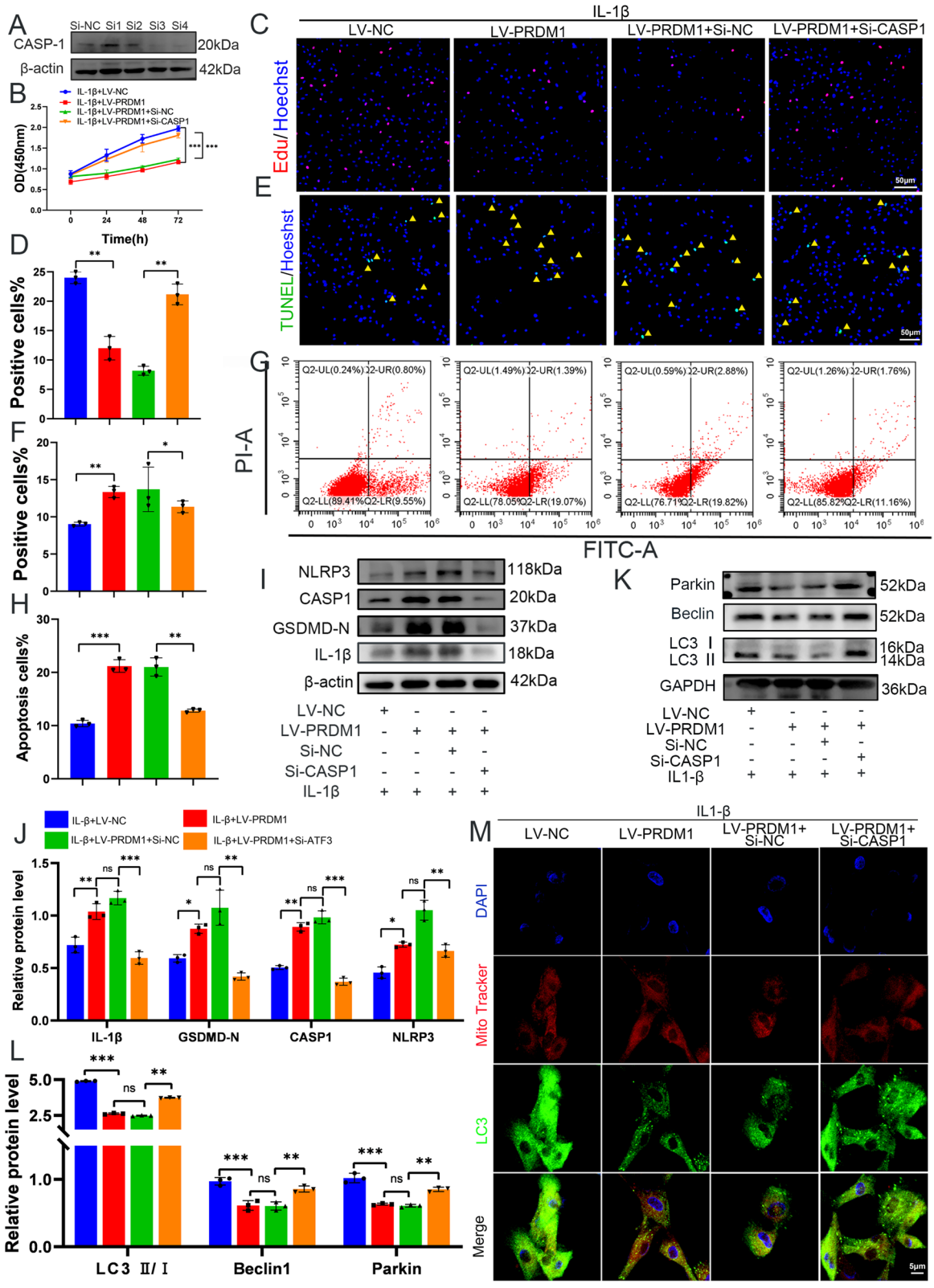
A
Si-NC Si1 Si2 Si3 Si4
CASP-1
20kDa
β-actin
42kDa
B
IL-1β+LV-NC
IL-1β+LV-PRDM1
IL-1β+LV-PRDM1+Si-NC
IL-1β+LV-PRDM1+Si-CASP1
OD(450nm)
Time(h)
C
IL-1β
LV-NC
LV-PRDM1
LV-PRDM1+Si-NC
LV-PRDM1+Si-CASP1
Edu/Hoechst
50μm
E
TUNEL/Hoechst
50μm
D
Positive cells%
F
Positive cells%
H
Apoptosis cells%
G
PI-A
FITC-A
Q2-UL(0.24%) Q2-UR(0.80%)
Q2-LL(89.41%) Q2-LR(9.55%)
Q2-UL(1.49%) Q2-UR(1.39%)
Q2-LL(78.05%) Q2-LR(19.07%)
Q2-UL(0.59%) Q2-UR(2.88%)
Q2-LL(76.71%) Q2-LR(19.82%)
Q2-UL(1.26%) Q2-UR(1.76%)
Q2-LL(85.82%) Q2-LR(11.16%)
I
NLRP3 118kDa
CASP1 20kDa
GSDMD-N 37kDa
IL-1β 18kDa
β-actin 42kDa
LV-NC
LV-PRDM1
Si-NC
Si-CASP1
IL-1β
K
Parkin 52kDa
Beclin 52kDa
LC3 I 16kDa
LC3 II 14kDa
GAPDH 36kDa
LV-NC
LV-PRDM1
Si-NC
Si-CASP1
IL1-β
J
IL-β+LV-NC
IL-β+LV-PRDM1
IL-β+LV-PRDM1+Si-NC
IL-β+LV-PRDM1+Si-ATF3
Relative protein level
IL-1β
GSDMD-N
CASP1
NLRP3
L
Relative protein level
LC3 Ⅱ/ Ⅰ
Beclin1
Parkin
M
IL1-β
LV-NC
LV-PRDM1
LV-PRDM1+ Si-NC
LV-PRDM1+ Si-CASP1
DAPI
Mito Tracker
LC3
Merge
5μm

◂**Fig. 7** PRDM1 promotes nucleus pulposus cell pyroptosis via activating CASP1 transcription. (**A**) Western blot detection of si-CASP1 silencing efficiency. (**B**) CCK-8 detects proliferative activity of LV-PRDM1 NPCs, which were transfected with si-NC or si-CASP1. (**C**, **D**) Edu detects proliferative activity of LV-PRDM1 NPCs transfected as in (B), scale bar, 50 μm. (**E**, **F**) TUNEL staining and statistical analysis results of TUNEL-positive cells, scale bar, 50 μm. (**G**, **H**) Flow cytometry analysis of the effects of CASP1 silencing on the death of LV-PRDM1NPCs. (**I**, **J**) Western blot detection and quantification of pyroptosis-related proteins (NLRP3, GSDMD-N, ASC, CASP1, IL-1β) of LV-PRDM1 NPCs transfected as in (B). (**K**, **L**) Western blot detection of mitophagy-related proteins (LC3, Parkin, Beclin1) of LV-PRDM1 NPCs transfected as in (B). (**M**) Immunofluorescence analysis of mitophagy staining in LV PRDM1 NPCs transfected as in (B), scale bar, 5 μm. $^{*}P<0.05$, $^{**}P<0.01$, $^{***}P<0.001$, NS not statistically significant

2018; Zheng et al. 2024). As a transcription factor, PRDM1 regulates downstream genes (Guo et al. 2022; Martins et al. 2008). Therefore, we hypothesized that PRDM1 regulates NPC mitophagy through its downstream target genes. To validate this hypothesis, sequencing results were analyzed in combination with hTFtarget and Chip-Atlas, and the potential target genes of PRDM1 and CASP1 were screened. We further confirmed that PRDM1 regulated CASP1 expression at both gene and protein levels. Subsequently, Chip and dual-luciferase reporter gene experiments demonstrated that PRDM1 binds to sites 1 (ATCTTTCTCTA) and 3 (CCTTTTCTCAT) in the *CASP1* promoter region. These results revealed that PRDM1 directly activated *CASP1* transcription to promote its expression. CASP1 inhibits mitophagy, triggers mitochondrial damage, exacerbating pyroptosis (Wang et al. 2020). Consistent with these results, the present study revealed that silencing of CASP1 reduced PRDM1-induced NPC death. Silencing of CASP1 reduced the induction of pyroptosis-related proteins (NLRP3, GSDMD-N, and IL-1β) by PRDM1 overexpression. Therefore, silencing CASP1 substantially reduced PRDM1-induced NPC pyroptosis. In addition, silencing of CASP1 promoted the expression of mitophagy-related proteins (LC3, Beclin1, and Parkin) and mitophagosome formation in NPCs, suggesting that silencing CASP1 reversed the inhibitory effect of PRDM1 on NPC mitophagy. Our findings demonstrated that PRDM1 inhibited mitophagy to promote NPC pyroptosis by directly activating CASP1 transcription.

This study had several limitations. First, owing to the lack of an animal model that fully recapitulates human IVDD, the rat disc puncture model used in this study may not reflect the mechanisms underlying human IVDD development. We plan to investigate the function of PRDM1 in primates in future research. Second, we directly injected PRDM1 lentivirus into rats to aggravate the progression of IVDD and subsequently explored drugs that inhibit the expression of PRDM1 for potential treatment of the disease. Third, although our results demonstrated that PRDM1 inhibited mitophagy, thereby aggravating

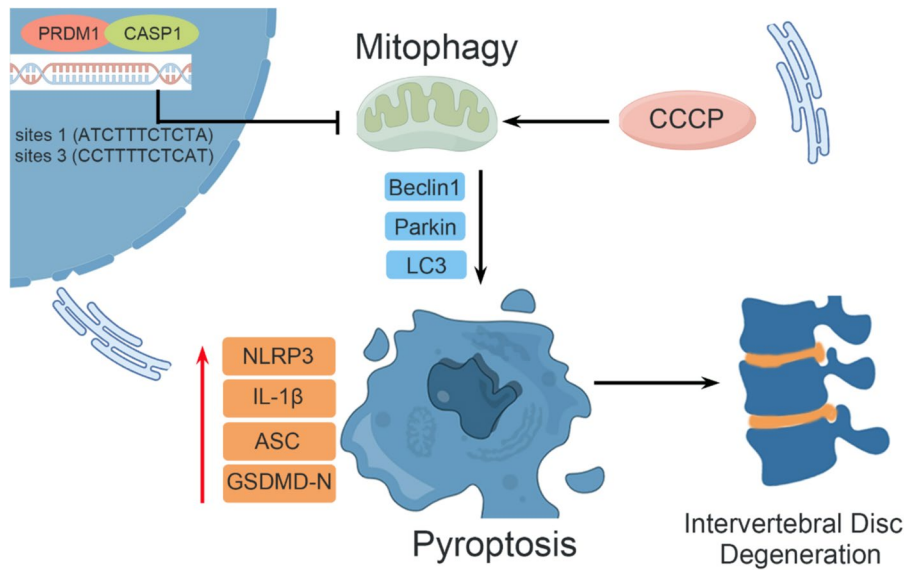

Fig. 8 Schematic illustration of the regulatory role of PRDM1 in IVDD progression

NPC pyroptosis by activating CASP1 transcription, the specific molecular mechanisms involved require further investigation.

In this study, we observed increased PRDM1 expression in degenerating NPCs. Regarding the molecular mechanisms, PRDM1 inhibited mitophagy by activating *CASP1* transcription, leading to NPC pyroptosis. In vivo experiments revealed that PRDM1 suppressed mitophagy to promote pyroptosis and exacerbate IVDD progression (Fig. 8). This study highlighted the role of PRDM1 in the pathogenesis of IVDD and suggests that PRDM1 could serve as a promising target for IVDD treatment.

Acknowledgements We thank the other partners of our laboratory for their helpful suggestions.

Author contributions Y. D. and C.Y. designed the research; C.Y., J.L. and W.K. performed theexperiments; C.Y., J.L., Y.C.and S.N. analyzed data; C.Y. and Y.D. wrote the manuscript. All authors reviewed the manuscript.

Funding This work was supported by National Natural Science Foundation of China, China (grant number 82274539), Natural Science Foundation of Guangdong, China (grant number 2023B1515120081).

Data availability No datasets were generated or analysed during the current study.

Declarations

Ethical approval The Animal Experimentation Center Committee of Zhujiang Hospital, Southern Medical University approved all animal experiments (LAEC-2023–121).

Conflicts of interest The authors declare no competing interests.

References

Chen J, Zhu S, Jiang N, Shang Z, Quan C, Niu Y. Hoxb3 promotes prostate cancer cell progression by transactivating cdca3. Cancer Lett. 2013;330(2):217–24. https://doi.org/10.1016/j.canlet.2012.11.051.

Clouet J, Fusellier M, Camus A, Le Visage C, Guicheux J. Intervertebral disc regeneration: from cell therapy to the development of novel bioinspired endogenous repair strategies. Adv Drug Deliv Rev. 2019;146:306–24. https://doi.org/10.1016/j.addr.2018.04.017.

Duan Y, Yu C, Kuang W, Li J, Qiu S, Ni S, et al. Mesenchymal stem cell exosomes inhibit nucleus pulposus cell apoptosis via the mir-125b-5p/traf6/nf-κb pathway axis. Acta Biochim Biophys Sin. 2023. https://doi.org/10.3724/abbs.2023241.

Fine N, Lively S, Séguin CA, Perruccio AV, Kapoor M, Rampersaud R. Intervertebral disc degeneration and osteoarthritis: a common molecular disease spectrum. Nat Rev Rheumatol. 2023;19(3):136–52. https://doi.org/10.1038/s41584-022-00888-z.

Francisco V, Pino J, Gonzalez-Gay MA, Lago F, Karppinen J, Tervonen O, et al. A new immunometabolic perspective of intervertebral disc degeneration. Nat Rev Rheumatol. 2022;18(1):47–60. https://doi.org/10.1038/s41584-021-00713-z.

Guo D, Cheng K, Song C, Liu F, Cai W, Chen J, et al. Mechanisms of inhibition of nucleus pulposus cells pyroptosis through sdf1/cxcr4-nfkb-nlrp3 axis in the treatment of intervertebral disc degeneration by duhuo jisheng decoction. Int Immunopharmacol. 2023;124:110844. https://doi.org/10.1016/j.intimp.2023.110844.

Guo H, Wang M, Wang B, Guo L, Cheng Y, Wang Z, et al. Prdm1 drives human primary t cell hyporesponsiveness by altering the t cell transcriptome and epigenome. Front Immunol. 2022;13. https://doi.org/10.3389/fimmu.2022.879501.

Han B, Zhu K, Li FC, Xiao YX, Feng J, Shi ZL, et al. A simple disc degeneration model induced by percutaneous needle puncture in the rat tail. Spine. 2008;33(18):1925–34. https://doi.org/10.1097/BRS.0b013e31817c64a9.

Kim J, Moon Y. Mucosal ribosomal stress-induced prdm1 promotes chemoresistance via stemness regulation. Commun Biol. 2021;4(1). https://doi.org/10.1038/s42003-021-02078-1.

Lai S, Phelps CA, Short AM, Dutta SM, Mu D. Thyroid transcription factor 1 enhances cellular statin sensitivity via perturbing cholesterol metabolism. Oncogene. 2018;37(24):3290–300. https://doi.org/10.1038/s41388-018-0174-7.

Lambert SA, Jolma A, Campitelli LF, Das PK, Yin Y, Albu M, et al. The human transcription factors. Cell. 2018;172(4):650–65. https://doi.org/10.1016/j.cell.2018.01.029.

Li Q, Zhang L, You W, Xu J, Dai J, Hua D, et al. Prdm1/blimp1 induces cancer immune evasion by modulating the usp22-spi1-pd-l1 axis in hepatocellular carcinoma cells. Nat Commun. 2022;13(1). https://doi.org/10.1038/s41467-022-35469-x.

Lin J, Du J, Wu X, Xu C, Liu J, Jiang L, et al. Sirt3 mitigates intervertebral disc degeneration by delaying oxidative stress-induced senescence of nucleus pulposus cells. J Cell Physiol. 2021;236(9):6441–56. https://doi.org/10.1002/jcp.30319.

Liu Z, Wang M, Wang X, Bu Q, Wang Q, Su W, et al. Xbp1 deficiency promotes hepatocyte pyroptosis by impairing mitophagy to activate mtdna-cgas-sting signaling in macrophages during acute liver injury. Redox Biol. 2022;52:102305. https://doi.org/10.1016/j.redox.2022.102305.

Liu Y, Dou Y, Sun X, Yang Q. Mechanisms and therapeutic strategies for senescence-associated secretory phenotype in the intervertebral disc degeneration microenvironment. J Orthop Transl. 2024;45:56–65. https://doi.org/10.1016/j.jot.2024.02.003.

Liu C, Banister CE, Weige CC, Altomare D, Richardson JH, Contreras CM, et al. Prdm1 silences stem cell-related genes and inhibits proliferation of human colon tumor organoids. Proc Natl Acad Sci. 2018;115(22). https://doi.org/10.1073/pnas.1802902115.

Luo T, Jia X, Feng W, Wang J, Xie F, Kong L, et al. Bergapten inhibits nlrp3 inflammasome activation and pyroptosis via promoting mitophagy. Acta Pharmacol Sin. 2023;44(9):1867–78. https://doi.org/10.1038/s41401-023-01094-7.

Lyu FJ, Cui H, Pan H, Mc CK, Cao X, Iatridis JC, et al. Painful intervertebral disc degeneration and inflammation: from laboratory evidence to clinical interventions. Bone Res. 2021;9(1):7. https://doi.org/10.1038/s41413-020-00125-x.

Ma Z, Tang P, Dong W, Lu Y, Tan B, Zhou N, et al. Sirt1 alleviates il-1β induced nucleus pulposus cells pyroptosis via mitophagy in intervertebral disc degeneration. Int Immunopharmacol. 2022;107:108671. https://doi.org/10.1016/j.intimp.2022.108671.

Ma J, Li Z, Xu J, Lai J, Zhao J, Ma L, et al. Prdm1 promotes the ferroptosis and immune escape of thyroid cancer by regulating usp15-mediated selenbp1 deubiquitination. J Endocrinol Invest. 2024. https://doi.org/10.1007/s40618-024-02385-4.

Martins GA, Cimmino L, Liao J, Magnusdottir E, Calame K. Blimp-1 directly represses il2 and the il2 activator fos, attenuating t cell proliferation and survival. J Exp Med. 2008;205(9):1959–65. https://doi.org/10.1084/jem.20080526.

Novais EJ, Diekman BO, Shapiro IM, Risbud MV. P16ink4a deletion in cells of the intervertebral disc affects their matrix homeostasis and senescence associated secretory phenotype without altering onset of senescence. Matrix Biol. 2019;82:54–70. https://doi.org/10.1016/j.matbio.2019.02.004.

Peng X, Zhang C, Zhou Z, Wang K, Gao J, Qian Z, et al. A20 attenuates pyroptosis and apoptosis in nucleus pulposus cells via promoting mitophagy and stabilizing mitochondrial dynamics. Inflamm Res. 2022;71(5–6):695–710. https://doi.org/10.1007/s00011-022-01570-6.

Pfirrmann CWA, Metzdorf A, Zanetti M, Hodler J, Boos N. Magnetic resonance classification of lumbar intervertebral disc degeneration. Spine Phila Pa 1976. 2001;26(17):1873–8. https://doi.org/10.1097/00007632-200109010-00011.

Samanta A, Lufkin T, Kraus P. Intervertebral disc degeneration—current therapeutic options and challenges. Front Public Health. 2023;11. https://doi.org/10.3389/fpubh.2023.1156749.

Song C, Cai W, Liu F, Cheng K, Guo D, Liu Z. An in-depth analysis of the immunomodulatory mechanisms of intervertebral disc degeneration. Jor Spine. 2022;5(4):e1233. https://doi.org/10.1002/jsp2.1233.

Song C, Xu Y, Peng Q, Chen R, Zhou D, Cheng K, et al. Mitochondrial dysfunction: a new molecular mechanism of intervertebral disc degeneration. Inflamm Res. 2023a;72(12):2249–60. https://doi.org/10.1007/s00011-023-01813-0.

Song C, Zhou Y, Cheng K, Liu F, Cai W, Zhou D, et al. Cellular senescence – molecular mechanisms of intervertebral disc degeneration from an immune perspective. Biomed Pharmacother. 2023b;162:114711. https://doi.org/10.1016/j.biopha.2023.114711.

Tam V, Chan W, Leung V, Cheah K, Cheung K, Sakai D, et al. Histological and reference system for the analysis of mouse intervertebral disc. J Orthop Res. 2018;36(1):233–43. https://doi.org/10.1002/jor.23637.

Wang X, Wang K, Han L, Zhang A, Shi Z, Zhang K, et al. Prdm1 is directly targeted by mir-30a-5p and modulates the wnt/β-catenin pathway in a dkk1-dependent manner during glioma growth. Cancer Lett. 2013;331(2):211–9. https://doi.org/10.1016/j.canlet.2013.01.005.

Wang X, Li H, Li W, Xie J, Wang F, Peng X, et al. The role of caspase-1/gsdmd-mediated pyroptosis in taxol-induced cell death and a taxol-resistant phenotype in nasopharyngeal carcinoma regulated by autophagy. Cell Biol Toxicol. 2020;36(5):437–57. https://doi.org/10.1007/s10565-020-09514-8.

Wang D, Zhang L, He D, Zhang Y, Zhao L, Miao Z, et al. A natural hydrogel complex improves intervertebral disc degeneration by correcting fatty acid metabolism and inhibiting nucleus pulposus cell pyroptosis. Mater Today Bio. 2024a;26:101081. https://doi.org/10.1016/j.mtbio.2024.101081.

Wang Z, Li X, Yu P, Zhu Y, Dai F, Ma Z, et al. Role of Autophagy and Pyroptosis in Intervertebral Disc Degeneration. 2024b;17:91–100. https://doi.org/10.2147/JIR.S434896.

Xia J, Chu C, Li W, Chen H, Xie W, Cheng R, et al. Mitochondrial protein ucp1 inhibits the malignant behaviors of triple-negative breast cancer through activation of mitophagy and pyroptosis. Int J Biol Sci. 2022;18(7):2949–61. https://doi.org/10.7150/ijbs.68438.

Xin J, Wang Y, Zheng Z, Wang S, Na S, Zhang S. Treatment of intervertebral disc degeneration. Orthop Surg. 2022. https://doi.org/10.1111/os.13254.

Xing H, Zhang Z, Mao Q, Wang C, Zhou Y, Zhou X, et al. Injectable exosome-functionalized extracellular matrix hydrogel for metabolism balance and pyroptosis regulation in intervertebral disc degeneration. J Nanobiotechnol. 2021;19(1). https://doi.org/10.1186/s12951-021-00991-5.

Yawoot N, Sengking J, Govitrapong P, Tocharus C, Tocharus J. Melatonin modulates the aggravation of pyroptosis, necroptosis, and neuroinflammation following cerebral ischemia and reperfusion injury in obese rats. Biochim

Biophys Acta Mol Basis Dis. 2023;1869(7):166785. https://doi.org/10.1016/j.bbadis.2023.166785.

Yu X, Wang Y, Lu R, Guo X, Qu Y, Wang S, et al. Bmp7 ameliorates intervertebral disc degeneration in type 1 diabetic rats by inhibiting pyroptosis of nucleus pulposus cells and nlrp3 inflammasome activity. Mol Med. 2023;29(1). https://doi.org/10.1186/s10020-023-00623-8.

Zhang W, Li G, Luo R, Lei J, Song Y, Wang B, et al. Cytosolic escape of mitochondrial dna triggers cgas-sting-nlrp3 axis-dependent nucleus pulposus cell pyroptosis. Exp Mol Med. 2022;54(2):129–42. https://doi.org/10.1038/s12276-022-00729-9.

Zhao Q, Xia N, Xu J, Wang Y, Feng L, Su D, et al. Pro-inflammatory of prdm1/sirt2/nlrp3 axis in monosodium urate-induced acute gouty arthritis. J Innate Immun. 2023;15(1):614–28. https://doi.org/10.1159/000530966.

Zhao K, An R, Xiang Q, Li G, Wang K, Song Y, et al. Acid-sensing ion channels regulate nucleus pulposus cell inflammation and pyroptosis via the nlrp3 inflammasome in intervertebral disc degeneration. Cell Prolif. 2021;54(1). https://doi.org/10.1111/cpr.12941.

Zheng H, Fang J, Lu W, Liu Y, Chen S, Huang G, et al. Tcf12 regulates the tgf-β/smad2/3 signaling pathway to accelerate the progression of osteoarthritis by targeting cxcr4. J Orthop Transl. 2024;44:35–46. https://doi.org/10.1016/j.jot.2023.11.006.

Zhong H, Li M, Wu H, Ying H, Zhong M, Huang M. Silencing ddx3 attenuates interleukin-1β-induced intervertebral disc degeneration through inhibiting pyroptosis. Inflammation. 2024. https://doi.org/10.1007/s10753-024-02042-1.

Zhou H, Qian Q, Chen Q, Chen T, Wu C, Chen L, et al. Enhanced mitochondrial targeting and inhibition of pyroptosis with multifunctional metallopolyphenol nanoparticles in intervertebral disc degeneration. Small. 2023a. https://doi.org/10.1002/smll.202308167.

Zhou K, Ran R, Gong C, Zhang S, Ma C, Lv J, et al. Roles of pyroptosis in intervertebral disc degeneration. Pathol Res Pract. 2023b;248:154685. https://doi.org/10.1016/j.prp.2023.154685.